CrossMark

ORIGINAL ARTICLE

Characterization of a potato activation-tagged mutant, *nikku*, and its partial revertant

Sukhwinder S. Aulakh · Richard E. Veilleux ·
Guozhu Tang · Barry S. Flinn

Abstract

Main conclusion **A potato mutant with a strong stress-response phenotype, and a partial mutant revertant, were characterized. Gene expression patterns and DNA cytosine methylation varied between these and wild-type, indicating a role for DNA cytosine methylation changes in the gene expression and visible phenotypes.**

Abstract Morphological and molecular studies were conducted to compare potato cv. Bintje, a Bintje activation-tagged mutant (*nikku*), and *nikku* revertant phenotype plants. Morphological studies revealed that *nikku* plants exhibited an extremely dwarf phenotype, had small hyponastic leaves, were rootless, and infrequently produced small tubers compared to wild-type Bintje. The overall phenotype was suggestive of a constitutive stress response, which was further supported by the greater expression level of several stress-responsive genes in *nikku*. Unlike the *nikku* mutant, the revertant exhibited near normal shoot elongation, larger leaves and consistent rooting. The reversion appeared partial, and was not the result of a loss of 35S enhancer copies from the original *nikku* mutant. Southern blot analyses indicated the presence of a single T-DNA insertion on chromosome 12 in the mutant. Gene expression studies comparing Bintje, *nikku* and revertant phenotype plants indicated transcriptional activation/repression of several genes flanking both sides of the insertion in the mutant, suggesting that activation tagging had pleiotropic effects in *nikku*. In contrast, gene expression levels for many, but not all, of the same genes in the revertant were similar to Bintje, indicating some reversion at the gene expression level as well. DNA methylation studies indicated differences in cytosine methylation status of the 35S enhancers between the n*ikku* mutant and its revertant. In addition, global DNA cytosine methylation varied between Bintje, the n*ikku* mutant and the revertant, suggesting involvement in gene expression changes, as well as mutant phenotype.

Abbreviations

5-mC	5-Methylcytosine
ABA	Abscisic acid
APX	Ascorbate peroxidase
CaMV	Cauliflower mosaic virus
CBF	C-repeat binding factor
COR	Cold regulated gene
IBA	Indole-3-butyric acid
LEA	Late embryogenesis abundant
P5CS	Pyrroline-5-carboxylate synthase
RMA1H1	RING membrane-anchor 1 homologue 1
T-DNA	Transfer DNA
Up	*Underperformer* (an activation-tagged potato mutant)
WRKY	WRKY (W = Tryptophan, R = Arginine, K = Lysine, Y = Tyrosine) domain

S. S. Aulakh · R. E. Veilleux · B. S. Flinn
Department of Horticulture, Virginia Tech, Blacksburg, VA 24060, USA

S. S. Aulakh · G. Tang · B. S. Flinn (✉)
Center for Sustainable and Renewable Resources (CSRR), Institute for Advanced Learning and Research (IALR), Danville, VA 24540, USA
e-mail: barry.flinn@ialr.org

Introduction

Mutagenesis remains a key strategy in the investigation of biological processes. Genetic mutants deficient or abundant in a biological process enable underlying gene(s) involved in the process to be identified and isolated. In agricultural species, mutagenesis has the added advantage of potentially creating agronomically useful phenotypes. The most widely used method is insertional mutagenesis, in which DNA elements such as transposons and T-DNA sequences are inserted into the genome, where they modify the function of a target gene and act as a molecular tag that can be useful for gene cloning (Ayliffe and Pryor 2007). Insertional mutagenesis is a useful approach for functional gene discovery, as is evident from the concentrated development of both loss-of-function and gain-of-function mutant populations for several plant species (Krysan et al. 1999; Suzuki et al. 2001; Ito et al. 2005; He et al. 2007; Miyao et al. 2007; Veilleux et al. 2012). Transcriptional enhancers derived from the cauliflower mosaic virus 35S RNA (35S CaMV) promoter were first used in plants in the T-DNA of a plasmid for *Agrobacterium*-based transformation of Arabidopsis to generate gain-of-function mutants (Hayashi et al. 1992); this strategy has become known as activation tagging. The most widely used constitutive promoter in many T-DNA cassettes for plant transformation was derived from the 35S CaMV promoter. Several activation tagging vectors were constructed or modified, which included transposons or other complex constructs, and these have been successfully used to discover gene functions in various plant species (Walden et al. 1994; Kardailsky et al. 1999; Borevitz et al. 2000; van der Graaff et al. 2000, 2003; Weigel et al. 2000; Suzuki et al. 2001; Jeong et al. 2002; Marsch-Martinez et al. 2002; Busov et al. 2003, 2011; Mathews et al. 2003; Ayliffe et al. 2007). A typical activation tagging vector has strong enhancer elements near one end of the T-DNA, theoretically to increase the expression of native genes located within a few kilobases of chromosomal DNA from the insertion site, thus producing a gain-of-function phenotype.

These mutant phenotypes are expected to be a consequence of altered gene function due to native gene overexpression rather than gene inactivation. The different mutation spectrum offered by this process has the potential for generating agronomically advantageous phenotypes previously unobtainable by conventional mutagenesis (Ayliffe et al. 2007). Enhancer or promoter sequences can potentially lead to different types of transcriptional perturbations and may produce novel phenotypes, which can aid in determining important gene functions.

In this paper, we present the results of the characterization of a potato mutant generated using activation tagging. This mutant was extremely dwarfed, slow growing, had hyponastic, rudimentary leaves and reduced apical dominance, produced either no or occasional small tubers, deficient in stem and leaf growth and rootless. Based on its phenotype, we named the mutant line 'nikku' (Hindi-little one). During routine subculture of *nikku* shoots growing in vitro, we observed some mutant phenotypic instability and revertant phenotype plant formation. The revertants formed functional roots, developed more prominent leaves and were larger than *nikku* plants. The revertant phenotype plants maintained their phenotype through subsequent subcultures. Morphological and molecular analyses of these revertant phenotype plants were performed and compared to the original *nikku* mutant and wild-type Bintje plants. The recent availability of the potato genome sequence (The Potato Genome Sequencing Consortium 2011) allowed us to localize the T-DNA insertion on chromosome 12, and identify flanking genes. Changes in expression of genes flanking the T-DNA were studied using semi-quantitative PCR and compared with Bintje, *nikku* and the revertant. We also examined the cytosine methylation status of 35S enhancer sequences, as well as global cytosine methylation in wild-type, mutant and revertant phenotype plants. We show that differential methylation at the local level of the inserted 35S CaMV enhancers, and differential methylation at the global level, was associated with differences in the observed phenotypes.

Materials and methods

Plant materials

The wild-type Bintje and activation-tagged line AT601 (*nikku*) mutant plantlets were initially generated by the Canadian Potato Genome Project (Regan et al. 2006), and maintained in culture as described previously (Aulakh et al. 2014). The revertant phenotype plants were first noticed after several generations of subculture and multiplication of *nikku* plants. The revertant phenotype plants were separated from the original mutant *nikku* plants and maintained separately. All plants were maintained on MS (Murashige and Skoog 1962) basal medium with vitamins (PhytoTechnology Labs, Lenexa, KS, USA) supplemented with 3 % sucrose, pH 5.8 and solidified with 0.7 % agar as control medium, referred to as PGM (Aulakh et al. 2014).

Determination of T-DNA copy number by Southern blot analysis and PCR

Genomic DNA was extracted using Plant DNAzol Reagent (Life Technologies, Grand Island, NY, USA) following

manufacturer's instructions. Genomic DNA of Bintje and *nikku* was digested with *Pci*I and *Psi*I restriction enzymes and separated on a 0.8 % agarose gel. PCR was used to determine 35S enhancer copy number in revertant phenotype plants. PCR analysis was performed using several sets of primers designed to amplify fragments of the pSKI074 T-DNA vector from genomic DNA. The primer sequences used in these PCR reactions are given in Suppl. Table S1. Each PCR reaction was performed in a total reaction volume of 20 µl, with 1–2 units of ExTaq DNA Polymerase (Takara Bio USA Inc., Madison, WI, USA) and 50–100 ng of DNA template in a MyCycler (Bio-Rad, Hercules, CA, USA) thermal cycler.

In vitro plant growth and tuberization

For in vitro plant growth assays, wild-type Bintje, the original *nikku* mutant and revertant phenotype plants were grown from 1 cm long explants (with at least one node) taken from 4- to 5-week-old in vitro plantlets. The experiment was conducted in a randomized block design with three replicates. Growth data were recorded after 4 weeks on plantlet growth medium PGM. For in vitro tuberization assays, stem sections, 3–5 cm in length, were treated as described previously (Aulakh et al. 2014).

Phenotyping under growth chamber and greenhouse conditions

Microtubers of Bintje, *nikku* and revertant phenotype plants produced during in vitro tuberization experiments were planted in 15 cm diameter pots filled with commercial Miracle-Gro® Potting Mix (ScottsMiracle-Gro, Marysville, OH, USA). Standard plant growth practices were followed. The greenhouse temperature setting was 24–30 °C and 16 h photoperiod was maintained by supplementary lighting with 1000 watt, 5.7 K daylight spectrum, metal halide bulbs. This growth experiment was done at the greenhouse of the Center for Sustainable and Renewable Resources (CSRR) at the Institute for Advanced Learning and Research (IALR), Danville, VA, USA.

Identification of potato genomic regions flanking the T-DNA

Regions flanking the T-DNA were amplified using the GenomeWalker universal kit (Clontech, Mountain View, CA, USA) as described previously (Aulakh et al. 2014). Recovered genomic sequences flanking the left border of the T-DNA insertion sites were identified and used to perform Basic Local Alignment Search Tool (BLAST) searches of the potato genome using the Spud DB Potato Genomics Resource (http://potato.plantbiology.msu.edu/

integrated_searches.shtml) with default search parameters (expected threshold 10, maximum number of alignments 100, max number of descriptions 100, word length 11, no filter and both strands). Approximately 700 kb of potato sequence from the right border and 400 kb from the left border of the T-DNA insertion site were analyzed for the presence of annotated gene models using the Spud DB Genome Browser (http://potato.plantbiology.msu.edu/cgi-bin/gbrowse/potato/). Sequence homology searches and analyses were performed using the NCBI BLAST server. Sequence alignments were carried out by the CLUSTALW2 (Larkin et al. 2007) method and using the EMBL server (http://www.ebi.ac.uk/Tools/msa/clustalw2/).

Extraction of RNA and reverse transcriptase PCR

RNA was extracted from 4-week-old in vitro plantlets. All tissues above the culture medium level were collected (leaves and stems, without roots) and immediately frozen in liquid nitrogen and stored at −80 °C until needed. RNA was extracted using either the Concert Plant RNA Reagent (Invitrogen, Carlsbad, CA, USA) following manufacturer's instructions, or a combination of Trizol Reagent (Invitrogen) extraction and the RNeasy Mini Kit (Qiagen, Valencia, CA, USA) purification, following manufacturer's instructions. Purified total RNA was treated using the DNA-free™ Kit (Ambion, Foster City, CA, USA) following the manufacturer's instructions. First strand cDNA was synthesized with SuperScript III (Invitrogen) using 1 µg of total RNA and following the supplier's protocol. After cDNA synthesis, the final volume was adjusted to 100 µl of diluted cDNA for each cDNA synthesis reaction. Reverse transcription polymerase chain reaction (RT-PCR) was performed using gene-specific primers, as mentioned in supplementary material (Suppl. Table S2). Equal amounts of cDNA were used in each reaction and *Solanum tuberosum* elongation factor 1-α (StEF1-α) gene expression was used as control. ExTaq DNA Polymerase (Takara Bio USA Inc.) was used in all amplification reactions. Gel images were acquired using an AlphaImager gel documentation system (ProteinSimple, San Jose, CA, USA).

ABA, NaCl and IBA assays

For in vitro plant stress assays, Bintje single-node explants were taken from 4- to 5-week-old plants. For abscisic acid (ABA) and salt (NaCl) stress experiments, we used PGM amended with ABA (5, 25, 100, 500 or 1000 µM) or NaCl (25, 50, 100, 200 or 500 mM) treatments. For indole-3-butyric acid (IBA) experiments, we used Bintje and *nikku* explants taken from 4- to 5-week-old in vitro plantlets. PGM medium was used as control and treatments consisted

of different levels of IBA (20, 50, 100 or 200 µM). Explants on these media were grown under 16 h photoperiod, 24 ± 1 °C and 70–100 µmol photons m^{-2}s^{-1} light intensity in a plant growth chamber and data were recorded after 4 weeks. All experiments consisted of three replications arranged in a randomized block design.

Methylated DNA enrichment

Methylated DNA was enriched using the EpiXplore Methylated DNA Enrichment Kit (Clontech) following the manufacturer's protocol, using Sau3AI-digested genomic DNA from Bintje, nikku and revertant phenotype plants. The enriched methylated DNA from the MBD2 protein/TALON magnetic beads complex was eluted twice with 200 µl of elution buffer, pooled and used for downstream PCR reactions. To perform PCR with the methylation-enriched DNA, we designed primers within the 35S enhancer sequence (Suppl. Table S1) with a PCR product size of 321 bp.

Potato global methylated DNA quantification

We used the MethylFlash Methylated DNA Quantification Kit—Colorimetric (Epigentek, Farmingdale, NY, USA)—to quantify global DNA methylation by specifically measuring levels of 5-methylcytosine (5-mC) in an ELISA-like microplate-based format, following the manufacturer's protocol. DNA from 4- to 6-week-old in vitro potato plants was extracted using Plant DNAzol Reagent (Life Technologies), with four plants pooled for each sample.

Zebularine growth assay

Nodal explants from Bintje, nikku and the revertant were taken from 4- to 5-week-old in vitro plants growing on PGM. This experiment consisted of five treatment levels [PGM + different concentrations (2, 5, 10, 15 and 20 µM) of zebularine] and control. Explants on these media were grown under 16 h photoperiod, 24 ± 1 °C and 70–100 µmol photons m^{-2}s^{-1} light intensity in a plant growth chamber and plant height and root length were measured after 4 weeks of growth on the specific medium. All experiments consisted of two replications applied in a randomized block design.

Results

Description of the nikku mutant and revertant

The potato cv. Bintje was used as the genetic background to generate the activation-tagged mutants. The nikku mutant was selected for further study due to its distinct

phenotype observed in vitro. In contrast to wild-type Bintje plants grown for 1 month, mutant plants displayed slow shoot growth, short internodes, small rudimentary leaves which exhibited hyponasty, and formed no roots and tubers (Fig. 1). Mutant plantlets were initially screened by polymerase chain reaction (PCR) using vector-specific primers (Suppl. Table S1) to confirm the presence of the T-DNA plasmid sequences in the plant (data not shown). After several generations of subculture on plantlet growth medium (PGM), some nikku plants formed roots, their leaves became less hyponastic and larger than the original nikku mutant and the stems grew longer (Fig. 1). As these plants were more similar to Bintje than nikku, we termed these phenotypically different plants as revertants. The revertant phenotype plants exhibited a phenotype which was intermediate between the original nikku mutant and wild-type Bintje. However, the revertant phenotype also differed from wild-type Bintje plants and appeared to present a case of partial reversion.

Determination of T-DNA copy number by Southern blot analysis

We performed Southern blot analysis, using two restriction enzymes (PciI and PsiI) that cut within the T-DNA region,

Fig. 1 Comparison of in vitro plants of Bintje, nikku mutant and nikku revertant. One centimeter nodal stem explants were grown on Murashige and Skoog (MS) basal medium with vitamins supplemented with 3 % sucrose. Plants were grown using 16 h photoperiod, 24 ± 1 °C and 70–100 µmol photons m^{-2}s^{-1} light intensity in a plant growth chamber. Pictures were taken after 4 weeks of growth. Scale bar = 1 cm

just left of the tetramerized enhancer sequences. Using a probe that corresponded to the enhancer region of pSKI074, we observed a strong, single hybridizing band in the *nikku* mutant for both the restriction enzymes, indicating the presence of a single T-DNA insertion in the mutant (Suppl. Fig. S1). Since revertant phenotype plants were vegetatively propagated from *nikku* mutants, it was expected that the T-DNA copy number and location were similar to the original *nikku* mutant; this assumption of similar location was later confirmed by sequencing PCR products amplified from genomic DNA of revertant phenotype plants spanning the plant/T-DNA junction (data not reported).

In vitro plant growth and tuberization experiments

We carried out in vitro growth and tuberization experiments to quantify differences between the growth habits of Bintje, *nikku* and revertant phenotype plants. We found that most revertant phenotype plants were morphologically different, in that they were bushier than *nikku* and Bintje plants (Fig. 1). Mutant *nikku* plants exhibited a mean stem length of 0.9 cm which was significantly less than the Bintje control (4.7 cm) and the revertant (4.1 cm) after 4 weeks of growth. As initially observed, the *nikku* mutant plants rarely developed roots. The mean number of revertant roots (7.5) was significantly greater than Bintje roots (4.7) and the rootless *nikku* plants (Fig. 2). We also observed a significantly greater number of axillary branches with the revertant than for Bintje and *nikku*. In vitro tuberization experiments were conducted to assess the tuberization ability of the *nikku* mutant. Tuberization in the mutant and revertant was poor. There was a little difference in tuber shape and size between revertant and *nikku* plants, and both formed tuber-like structures which were smaller in size than round Bintje tubers (Fig. 3). The mean

number of tubers/explant (0.8) and weight of tubers/explant (0.2 g) for the revertant were not significantly different from *nikku* (number of tubers = 0.2 and weight of tubers = 0.04 g), but were significantly less than Bintje (number of tubers = 2.4 and weight of tubers = 2.3 g). However, the mean number of stolons/explant in the revertant (3.2) was significantly greater than *nikku* (0.7) and Bintje (0.2) explants (Fig. 4). Additionally, during the tuberization experiment, revertant phenotype plants expressed various degrees of reversion (Suppl. Fig. S2). As cytokinin is known to impact tuberization, we assessed the effects of kinetin on in vitro tuberization with both Bintje and *nikku*. In vitro tuberization using tuberization medium supplemented with 10 μM kinetin improved the number and weight of tubers for Bintje, but there was no effect on *nikku* tuberization (data not reported).

The *nikku* phenotype is associated with a constitutive stress response

The dwarf, slow-growing mutant phenotype resembled that of a constitutive stress response. To assess this, we used RT-PCR analysis to investigate the expression of several known stress-induced genes (See Suppl. Table S2 for primers used) with in vitro-grown Bintje and *nikku* shoots (Fig. 5). The transcript levels of four genes correlated with stress response were elevated in the *nikku* mutant. These genes include an AP2 domain CBF protein (PGSC0003DMG400014310; DMT400037121) gene encoding a cold-induced transcription factor, a dehydrin/LEA gene (PGSC0003DMG400009968; DMT400025812), P5CS (PGSC0003DMG402026767; DMT400068829; encoding the proline biosynthetic enzyme Δ1-pyrroline-5-carboxylate synthase), and an ascorbate peroxidase-encoding gene (PGSC0003DMG400030063; DMT400077286). Of these genes, the strongest induction in the mutant occurred with the P5CS gene.

In vitro assays with Bintje to recapitulate the mutant phenotype

Several experiments were conducted with Bintje explants in an attempt to recapitulate the mutant phenotype. As stress responses are often mediated through ABA, and several of the stress-associated genes listed above are induced by ABA, we subjected Bintje plantlets to in vitro growth in the presence of various concentrations of ABA (Suppl. Fig. S3 and Suppl. Fig. S4). We observed that increasing concentrations of ABA decreased stem length, leaf size and rooting (Suppl. Fig. S3). A concentration of 5 μM ABA reduced stem length threefold (2.8 cm) compared to the control treatment (8.5 cm), with increasing concentrations displaying further reduction (Suppl. Fig. S4). Root length was also significantly reduced (0.42 cm)
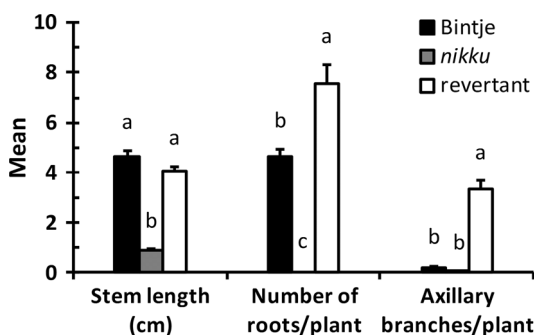

Fig. 2 In vitro plant growth data for Bintje, *nikku* mutant and *nikku* revertant. Data were recorded following 4 weeks of growth. The values are mean ± SE ($n = 13$). Statistical differences were calculated by one-way ANOVA. *Different letters* indicate means that were statistically different by Tukey's HSD multiple testing method ($P < 0.05$) for genotypes within a given growth parameter
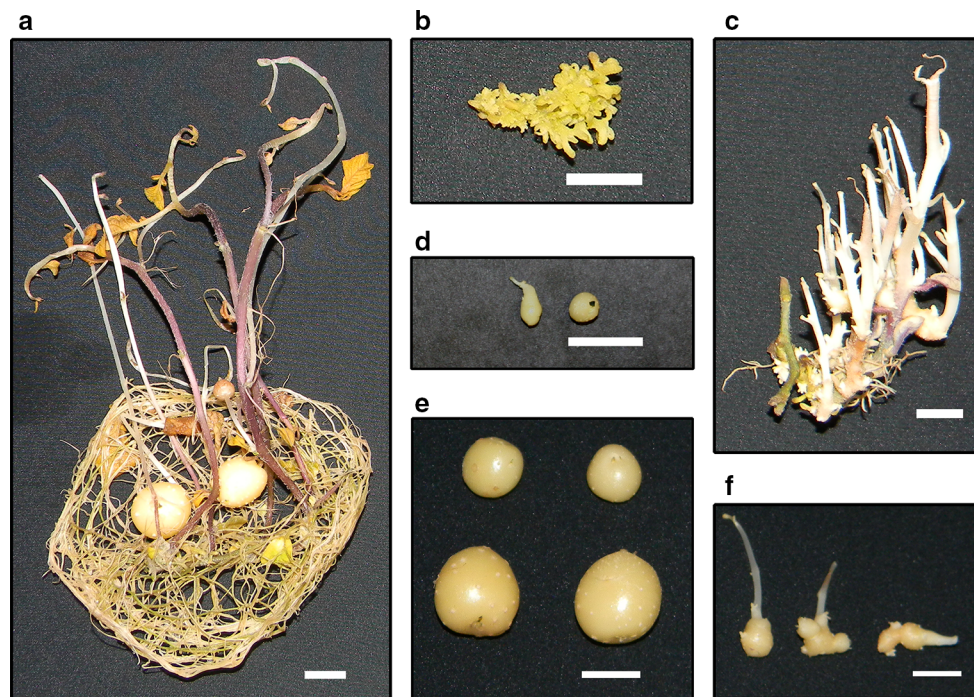
Fig. 3 In vitro tuberization. Bintje (**a**), *nikku* (**b**) and *nikku* revertant (**c**) explants after 30 days of growth in tuberization medium. Harvested tubers of *nikku* (**d**), Bintje (**e**), and *nikku* revertant (**f**) at the end of the tuberization experiment. Stem sections of 3–5 cm in length were grown in 40 ml liquid propagation medium at 24 ± 1 °C, 16 h photoperiod and 70–100 μmol photons m^{-2}s^{-1} light intensity for 4 weeks followed by 30 days of plant culture in microtuberization medium at 18–20 °C in the dark. *Scale bar* = 1 cm
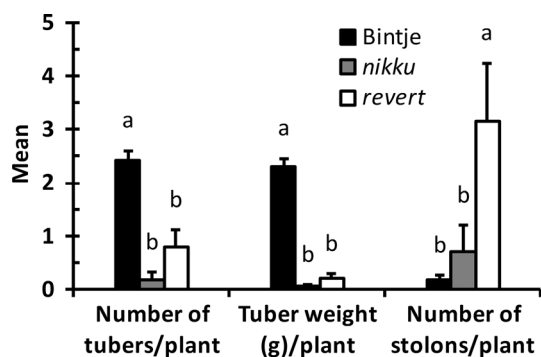

Fig. 4 Growth responses during in vitro tuberization for Bintje, *nikku* and *nikku* revertant. Data were recorded 30 days after culture on tuberization medium. The values are mean ± SE ($n = 24$). Statistical differences were calculated by one-way ANOVA. *Different letter*s indicate means that were statistically different by Tukey's HSD multiple testing method ($P < 0.05$) for genotypes within a given growth parameter. *Revert* revertant

Fig. 5 The *nikku* phenotype is associated with a constitutive stress response. Reverse transcriptase PCR analysis of various stress-induced genes for in vitro-grown Bintje and *nikku*. RNA was extracted from in vitro plantlets (leaves + stem). StEF1-α transcript expression was used as control

with 25 μM ABA compared to control treatment (4 cm). At the highest levels of ABA tested (500-1000 μM), the wild-type explants appeared similar to the *nikku* mutant. We also exposed Bintje explants to a salt stress assay, to assess similarity of the stressed plants to the *nikku* phenotype. At 25 mM NaCl, little effect was observed on stem length, root length and root number compared to control medium (Su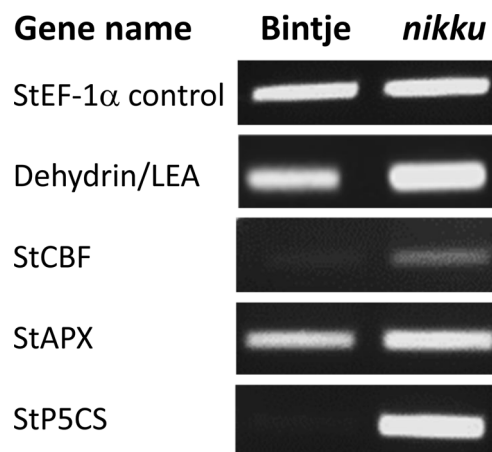ppl. Fig. S5 and Suppl. Fig. S6). However, greater levels of salt stress (>50 mM) significantly reduced all the observed traits; plants were significantly dwarfed and rootless at 200 mM NaCl, and died at 500 mM NaCl. Of the ABA and NaCl treatments, the ABA-treated Bintje explants at the highest concentrations tested appeared the most similar to the *nikku* phenotype.

Attempts at ex vitro growth characterization of *nikku* and the revertant

Due to the lack of rooting with *nikku* shoots, all of the growth data obtained were from in vitro experiments. In an attempt to generate consistently rooted plantlets for subsequent ex vitro growth experiments, we tested various concentrations of auxin (IBA) with *nikku* shoots (Suppl. Fig. S7). Our experimental treatments represented 0, 20, 50, 100 and 200 µM IBA, which were tested with both Bintje and *nikku* shoots. In the case of wild-type Bintje shoots, which rooted in the absence of any supplied auxin, increasing IBA concentrations greater than 50 µM significantly reduced root growth, and induced some basal callus formation in the root region (Suppl. Fig. S7 a-e). There was a stimulation of root number at 20 µM IBA. The *nikku* shoots also displayed increased basal callusing and additional dwarfing. In no cases, were any roots induced by the IBA treatment (Suppl. Fig. S7 f-j) with *nikku* shoots. Attempts were also made to graft *nikku* scions onto Bintje rootstocks via in vitro grafting, but the grafts were not able to take. However, we were able to grow a limited number of mutant plants (2) from the in vitro tubers produced earlier. Mutant shoots from the tubers maintained their slow growth phenotype ex vitro in soil, and no roots were formed. Little increase in stem length was observed over a period of 8 months, such that they still remained significantly smaller than Bintje plants grown from tubers (Fig. 6). In contrast to the typical compound leaves of potato (Fig. 6a), we noticed that the small-sized leaves of the mutant plants were simple (Fig. 6b). After 8 months, plants were discarded and the few small-sized tubers that could be harvested were much smaller and knobbier than the tubers from 3-month-old Bintje (Fig. 6c–d).

Some revertant phenotype plants were grown under greenhouse conditions from microtubers and compared with similarly propagated Bintje plants (Fig. 6e). The revertants had larger terminal leaves without lateral leaflets, resulting in a simple leaf compared to the typical compound leaf of wild-type Bintje (Fig. 6f). The petioles of the revertant were shorter and the rachis was absent. Additionally, leaf trichomes appeared more prominent in revertant phenotype plants than Bintje. We also observed differences in tuber set and tuber yield between Bintje and the revertant (data not reported). Hence, the partial reversion nature of the revertant remained consistent.

Identification of potato genomic regions flanking the T-DNA

To identify the location of the integrated T-DNA, we used GenomeWalker (Clontech) technology to isolate the genomic region flanking the T-DNA insertion (Suppl. Fig.
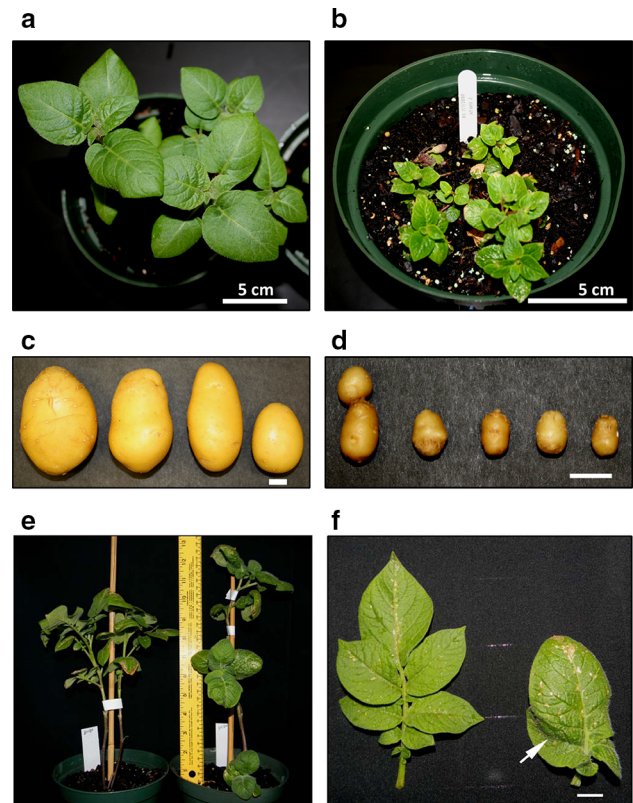

Fig. 6 Potato phenotyping under greenhouse conditions. Fifteen-day-old Bintje plant (**a**) and 8-month-old *nikku* plant (**b**) grown from microtubers. Bintje tubers harvested after 3 months of growth (**c**) and *nikku* tubers harvested from 8-month-old plants (**d**). Bintje (*left*) and revertant (*right*) plants grown from microtubers (**e**). These microtubers were produced during in vitro tuberization experiments and were planted in soil after breaking dormancy. Potato leaf phenotypes under greenhouse conditions (**f**). Typical compound leaf of potato cv. Bintje with oval lateral leaflets (*left*) and simple leaf of revertant without lateral leaflets (*right*). Leaves were taken from corresponding Bintje and revertant plants shown in **e**. *Arrows* indicate the difference in trichomes and the point of fusion between terminal leaf and lateral leaflets in the revertant leaf. *Scale bar* in **c**, **d** and **f** = 1 cm

S8). Sequences obtained using GenomeWalker were queried against the PGSC *S. tuberosum* group Phureja DM1-3 Pseudomolecules v4.03 database (revised on 10-10-2014). The T-DNA was located on chromosome 12 at genomic location 1824787 (Fig. 7). Further PCR and sequence analysis of the left border T-DNA/plant DNA junction site revealed that a vector backbone of 278 bp (7777–8053 sequence of vector pSKI074) outside of the T-DNA was also found in the *nikku* mutant. A similar analysis of the right border T-DNA/plant DNA junction site in the *nikku* mutant revealed no backbone T-DNA sequence integration (See Suppl. Table S1 for primers used). The recent availability of the potato genome sequence (The Potato Genome Sequencing Consortium 2011) allowed us to identify several gene model predictions on both sides of the T-DNA insertion. The first predicted open
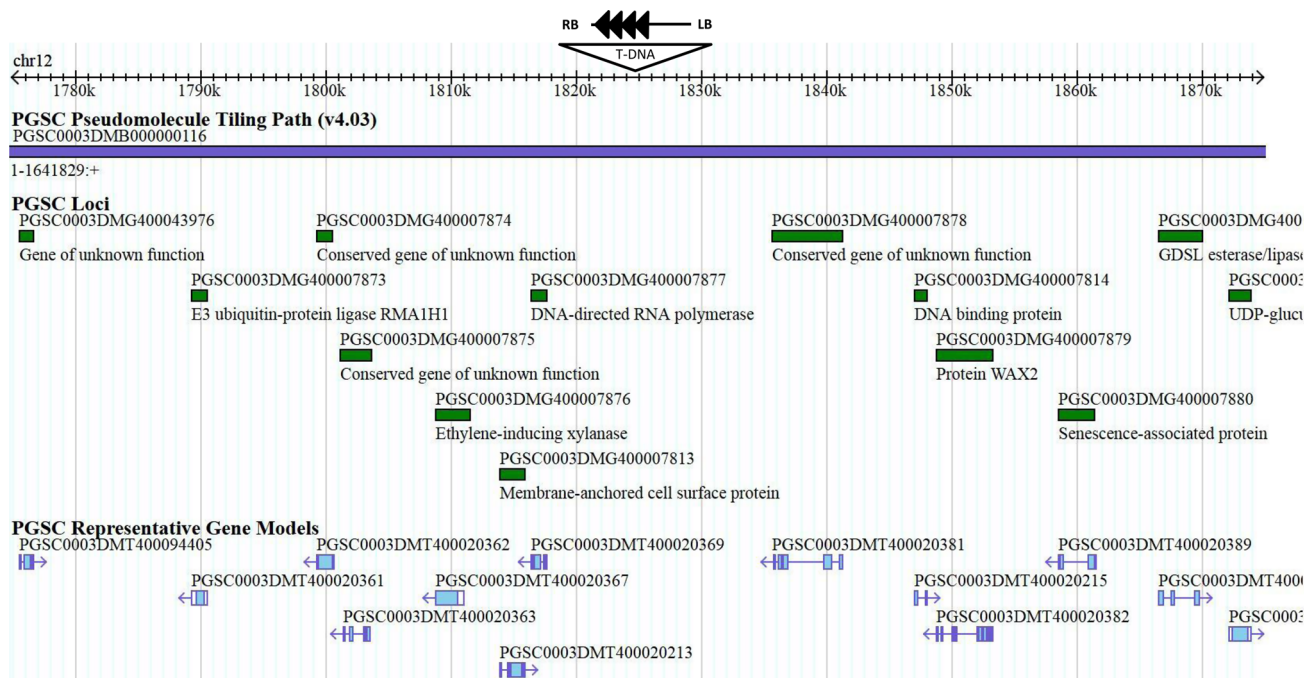
Fig. 7 Identification of potato genomic regions flanking the T-DNA insertion in the *nikku* mutant. A screen shot of a 100 kb region of chromosome 12 of the genome of doubled monoploid *S. tuberosum* Group Phureja clone DM1-3 (DM), showing the T-DNA insertion site and the flanking gene prediction models

reading frames flanking the T-DNA was approx. 7.2 and 10.8 kb from the right and left borders, respectively, of the T-DNA (Fig. 7).

Comparison of gene transcripts flanking the T-DNA in Bintje, *nikku* and revertant phenotype plants

Transcript analysis of several potato genes flanking the T-DNA insertion was performed using reverse transcriptase PCR (RT-PCR), with primers (Suppl. Table S2) designed against the reading frame for the various gene model predictions. We analyzed an approx. 700 kb potato genomic region flanking the right border (Fig. 8a) and an approx. 400 kb region off of the left border of the insertion site (Fig. 8b), and observed up- or down-regulation of various potato genes flanking both borders of the T-DNA. The expression levels of many genes, which were up-regulated in *nikku* were lower in the revertant, and were similar to levels found in Bintje. Similarly, expression levels of two genes (ethylene-inducing xylanase and senescence-associated protein) which were down-regulated in *nikku* plants, were more highly expressed in the revertant, and again were similar to the levels found in Bintje. Amongst the genes flanking the right border, the gene closest to the insertion was DNA-directed RNA polymerase, which showed little change in expression between Bintje and *nikku*. However, a subsequent gene, ethylene-

inducing xylanase, showed some down-regulation in the mutant. Several of the genes downstream from here showed increased expression in *nikku*, including a conserved gene of unknown function, an E3 ubiquitin ligase RMA1H1, a ribosomal protein alanine (referred to as NAT due to its homology with Acyl-CoA N-acyltransferase) and a predicted sugar transporter (referred as PMT, due to its homology with polyol/monosaccharide transporters), a receptor-like kinase SRF3 and a WRKY transcription factor (Fig. 8a). We also assessed the expression patterns in the leaves for several genes situated within 400 kb genomic region flanking the left border. One gene, encoding a senescence-associated protein, was observed to be down-regulated in the mutant. Several other genes displayed some up-regulation in the mutant, such as a GDSL esterase/ lipase gene, a serine–threonine protein phosphatase, a conserved gene of unknown function, and a DNA-binding protein phosphatase 2C (Fig. 8b). However, there was no apparent change in expression level for three genes (a vacuolar cation/proton exchanger, a DNA-binding protein phosphatase 2C and a CBL-interacting protein kinase 7) between Bintje, *nikku* and revertant. Therefore, the patterns of gene expression in Bintje and the revertant were generally similar, and differed from *nikku*. However, based on the patterns of gene expression observed near the T-DNA insertion site in *nikku*, we were unable to determine a single "tagged" gene.

Fig. 8 Comparison of various gene transcripts flanking the T-DNA insert in Bintje, *nikku* and revertant. **a** Gene transcripts flanking the right border of the T-DNA insert. **b** Gene transcripts flanking the left border of the T-DNA insert. Reverse transcriptase PCR analysis was done using gene-specific primers (Suppl. Table S2). RNA was extracted from in vitro plantlets (leaves + stem). The direction of the *arrow* indicates the orientation of the predicted transcript

a Gene identifier PGSC0003DMG	Gene annotation based on potato genome	Direction of transcript & distance from insert (kb)		Reverse transcriptase PCR (RNA from *in vitro* plants)		
				Bintje	*nikku*	revertant
Control	*S.tuberosum* elongation factor 1-α (EF1-α)					
400007877	DNA-directed RNA polymerase	⇐	8			
400007876	Ethylene-inducing xylanase	⇐	14			
400007875	Conserved gene of unknown function	⇐	21			
400007874	Conserved gene of unknown function	⇐	25			
400007873	E3 ubiquitin-protein ligase RMA1H1	⇐	34			
400007872	NBS-LRR protein	⇐	67			
400007868	Ribosomal-protein-alanine	⇐	115			
400007865	Sugar/Polyol monosaccharide transporter	⇐	170			
400007812	Conserved gene of unknown function	⇒	174			
400007811	Conserved gene of unknown function	⇒	201			
400007862	SRF3	⇐	225			
400007792	Vacuolar cation/proton exchanger	⇒	572			
400046891	Glucose-1-phosphate adenylyltransferase	⇒	595			
400007788	WRKY transcription factor	⇒	661			
400007786	2,4-D inducible glutathione S-transferase	⇒	699			
400007843	Ethylene receptor 1	⇐	703			

b Gene identifier PGSC0003DMG	Gene annotation based on potato genome	Direction of transcript & distance from insert (kb)		Reverse transcriptase PCR (RNA from *in vitro* plants)		
				Bintje	*nikku*	revertant
Control	*S.tuberosum* elongation factor 1-α (EF1-α)					
400007880	Senescence-associated protein	⇐	33			
400007815	GDSL esterase/lipase	⇒	41			
400007884	Serine/threonine-protein phosphatase	⇐	81			
400007818	Conserved gene of unknown function	⇒	88			
400007819	DNA-binding protein phosphatase 2C	⇒	108			
400007825	Translation initiation factor	⇒	340			
400007899	CBL-interacting protein kinase 7	⇐	404			

Determining the presence of 35S enhancers in the revertant

To assess for potential loss of 35S enhancers in the revertant, we amplified different T-DNA components of revertant genomic DNA by PCR. The T-DNA fragments amplified near the right border of pSKI074, using revertant genomic DNA and primers designed from T-DNA sequences (Suppl. Table S1) were identical in size and sequences to those of *nikku* and these fragments were amplified across the tetramer enhancers (Fig. 9a, b). Similarly, PCR with primers designed near the left border of the T-DNA also produced identical size gel bands with both revertant and *nikku* genomic DNA (Suppl. Table S1 and Fig. 9c). Therefore, it appears that revertant phenotype

plants still harbored the complete T-DNA without loss of enhancer copies. Collectively, these results suggest that the T-DNA structure, size, sequence and position within the genomes of *nikku* and revertant were unchanged.

Differential methylation of local 35S enhancer sequences in *nikku* and revertant

Having shown that the 35S tetramerized enhancer was intact in the revertant, we pursued another possible explanation underlying the phenotypic variation between *nikku* and the revertant; that DNA methylation of the 35S enhancers between the two plant types was different. Numerous potential methylation sites were present within the tetramerized 35S enhancer sequences (data not shown).
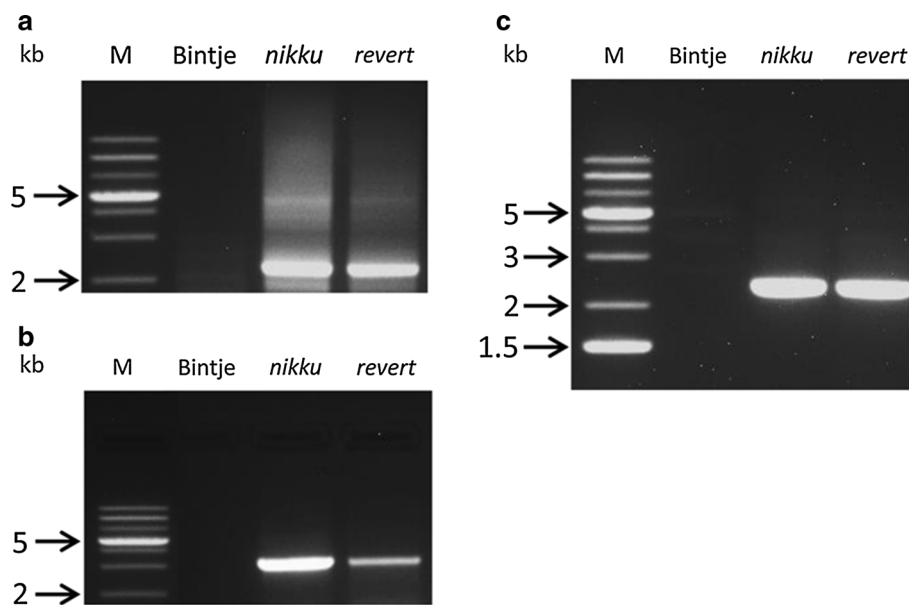
Fig. 9 Assessing the presence of T-DNA in the revertant (revert). PCR products were amplified from genomic DNA of the revertant to amplify right border (**a**, **b**) and left border (**c**) T-DNA fragments. Bintje and *nikku* genomic DNA was used as templates for negative and positive control reactions, respectively. Primer sequences used in **a** [AT set4-5′ and pSKI074-35S promoter-3′ (2232 bp)], **b** [pSKI074Fred-5′ and ATset4-3′ (3294 bp)] and **c** [pSKI074-8068..0.8090-5′ and pSKI074Red-3′ (2318 bp)] are given in Suppl. Table S1. *Numbers in small parentheses* above are the expected product sizes. *M* gene ruler 1 kb Plus DNA mass ladder

To assess cytosine methylation, we used a methylated DNA enrichment method, followed by PCR amplification of the 35S enhancers from the enriched fraction, to assess cytosine methylation levels of these enhancer DNA sequences in *nikku* and the revertant. The restriction enzyme *Sau*3AI was used to digest genomic DNA for the different samples, after which methylated DNA was selected on magnetic beads using an attached methylated DNA-binding protein. The methylated DNA fraction bound to the beads was eluted, and used for PCR of methylation-enriched DNA with 4x 35S *Sau*3AI primers (Suppl. Table S1) designed to amplify individual 321 bp enhancer sequences. We consistently observed fewer PCR products from the revertant than for *nikku*, even though equal amounts of methylation-enriched DNA were used as template (Fig. 10). These PCR results suggested 35S enhancer sequence hyper-methylation in the *nikku* mutant compared to the revertant. However, based on the methodology of this assay, we do not know what site-specific variation in cytosine methylation may exist between *nikku* and the revertant, and what contribution this could make in the modification of gene expression between the two.

Potato global methylated DNA quantification

The biological importance of 5-methylcytosine (5-mC) as a major epigenetic modification in phenotype and gene expression is well known. The indication of cytosine
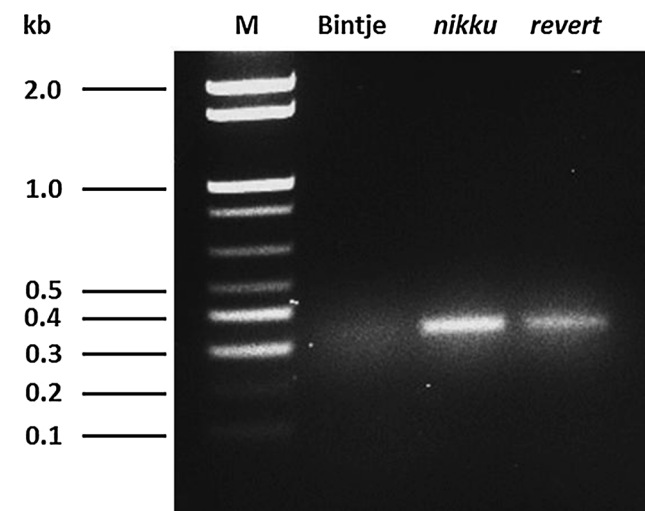

Fig. 10 Differential methylation status of 35S enhancers in *nikku* and revertant. Genomic DNA of *nikku* and revertant plants digested with restriction enzyme *Sau*3AI was enriched for cytosine methylated fragments (see "Materials and methods") and equal amounts of enriched DNA were used as template for PCR. Sequences of primers (35X4S *Sau*3AI- 5′ and 35X4S *Sau*3AI- 3′) are given in Suppl. Table S1. *M* Invitrogen 1 kb Plus DNA mass ladder

methylation differences in the 35S enhancers between *nikku* and the revertant led us to assess the global level of cytosine methylation in Bintje, *nikku* and the revertant. We used the MethylFlash Methylated DNA Quantification Kit to quantify 5-mC levels, and found that the 5-mC level of
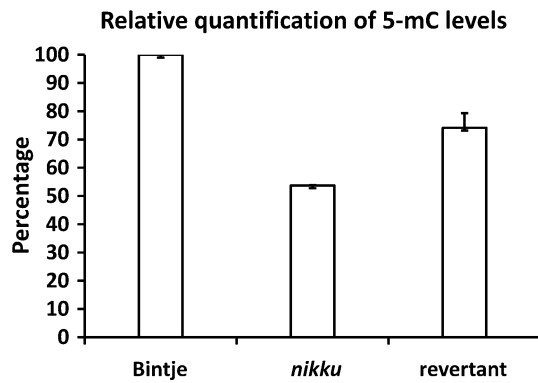
Relative quantification of 5-mC levels

Fig. 11 Relative quantification of 5-mC levels using MethylFlash Methylated DNA Quantification Kit. Quantification levels of *nikku* and revertant are expressed as relative percentage of Bintje methylation levels. For each sample, 100 ng DNA from 4- to 6-week-old in vitro potato plants were used

the revertant was greater than *nikku*, but lower than Bintje. More specifically, using Bintje as the standard, we found that the 5-mC level for *nikku* was approximately 50 % that of Bintje, whereas the revertant was 75 % of the Bintje 5-mC level, placing revertant 5-mC levels intermediate between the level of wild-type Bintje and mutant *nikku* 5-mC levels (Fig. 11), further indicating the partial phenotype of the revertant.

Artificial manipulation of DNA methylation levels using zebularine

To determine if the artificial manipulation of DNA cytosine methylation would result in Bintje explants recapitulating the *nikku* visual phenotype, we used the DNA methyltransferase inhibitor, zebularine. Zebularine treatments were applied to Bintje, *nikku* and revertant phenotype plants in vitro, and resulted in the stunting of explants. In terms of plant height, the largest reduction in growth was observed with Bintje, followed by revertant and then *nikku* plants. A similar growth inhibition trend was observed for root length. Increasing the zebularine concentration above 10 µm did not further reduce the plant height or root length. At the 10 µm level, the observed phenotypes resembled each other (Fig. 12a, b). Therefore, the artificial reduction of DNA cytosine methylation through the use of zebularine was able to reduce the growth phenotype of both Bintje and revertant to something similar to *nikku*, but had little effect on the *nikku* phenotype.

Discussion

This report describes the isolation and characterization of a potato activation-tagged mutant, *nikku*, which was identified by its extreme dwarf and lack of rooting phenotype, as well as small hyponastic leaves and little-to-no tuberization. These characteristics suggested a constitutive stress response, as is often reported for plants showing a severe dwarf phenotype (Williams et al. 2005; Jungkunz et al. 2011). Our application of stress treatments to wild-type Bintje nodal sections, through high levels of ABA and NaCl, generated similar dwarf phenotypes. In addition, it has been reported that tuber production during stress situations is greatly reduced, and the tubers were smaller in size (Silva et al. 2001), similar to our observations during *nikku* tuberization experiments. Furthermore, several types of genes known to be up-regulated under stress conditions (LEA, APX, CBF and P5CS) were expressed at greater levels in *nikku* compared to wild-type Bintje. All of these observations taken together suggest that the *nikku* phenotype is representative of a strong, constitutive stress response.

The stress-response genes described above and shown to be expressed at greater levels in *nikku* are known to be up-regulated by the plant stress-response growth regulator ABA. In the present study, application of various levels of ABA to wild-type Bintje nodal sections reconstituted a phenotype similar to that of the *nikku* mutant, namely lack of shoot, root and leaf growth. These results, along with the knowledge that ABA is known to reduce microtuber size (Gopal et al. 2004), suggest the involvement of components of the ABA signaling pathway as part of this constitutive stress response. While we did not analyze endogenous ABA content in *nikku* tissues, a comparison of ABA content between *nikku* and Bintje would be informative.

Our analysis of the chromosome sequences flanking the insertion site revealed that various genes flanking both ends of the T-DNA were modified in expression patterns compared to wild-type Bintje. Similar observations of gene expression modifications flanking either the left border or right border of the T-DNA insertion have been reported with other activation-tagged mutants (Imaizumi et al. 2005; Ahn et al. 2007; Hsing et al. 2007; Aulakh et al. 2014). Ahn et al. (2007) noted that while the gene adjacent to the enhancers was often activated, broad regions of the chromosome could be impacted by the 35S enhancers, and that any gene within that broad region, and not simply the gene immediately adjacent to the T-DNA, could be responsible for the dominant plant phenotype. This long distance modification of gene expression may not be surprising, as the chromatin structure surrounding the enhancer insertion site can strongly facilitate enhancer action over large DNA distances (Rubtsov et al. 2006).

Our previous analysis of a different Bintje activation-tagged mutant (*underperformer*) revealed a strong activation of the gene immediately adjacent to the enhancers
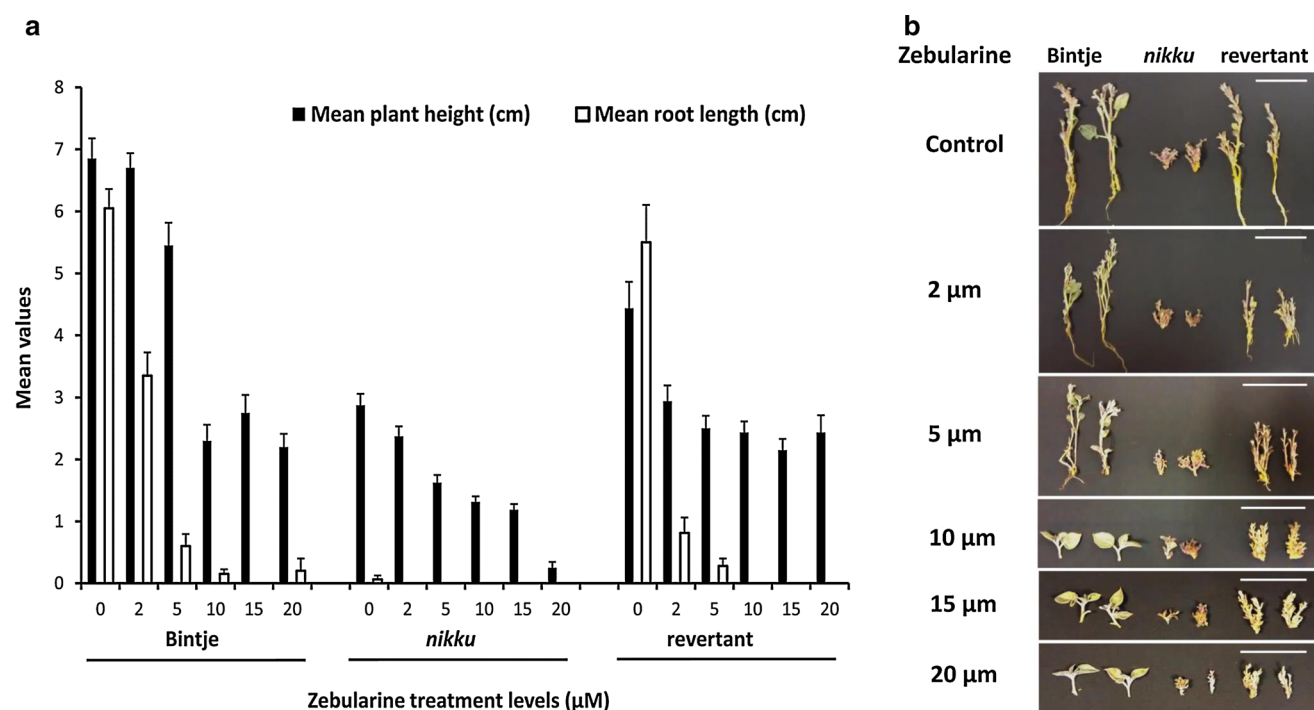
a

b

Fig. 12 Treatment with methylation inhibitor zebularine. **a** Plant growth data for Bintje, *nikku* mutant and *nikku* revertant plants. **b** Phenotypic effects of treatment with methylation inhibitor zebularine. Data and plant phenotypes were recorded following 1 month of growth on media containing different levels of zebularine. The values are mean ± SE ($n = 10$). Statistical differences were calculated by one-way ANOVA

(Aulakh et al. 2014). However, our results with *nikku* revealed no similar enhancement in the expression of the gene immediately adjacent to the right border of the enhancers, although several genes located from 34 to 703 kb downstream of the enhancer sequences showed up-regulation in *nikku*. In addition, our analyses indicated that various genes located from 40 to 106 kb off of the T-DNA left border exhibited up-regulation in the mutant, while one gene 33 kb from the left border appeared to be down-regulated in the mutant. These results agree with the comments by Ahn et al. (2007), indicating gene expression along a broad range of the chromosome being affected by the T-DNA insertion. Based on our initial analyses, a clear suggestion for the "tagged" gene was not deduced with the *nikku* mutant.

Regarding the activation tagging process, most studies have suggested that the genes downstream of the enhancer sequences are associated with the mutant phenotype, although determining the major contributor to the mutant phenotype may be more difficult to assess (Ahn et al. 2007). We noted that various genes on chromosome 12 were modified in their expression patterns in the *nikku* mutant. Several up-regulated genes downstream of the 35S enhancers encode proteins associated with stress responses, including an RMA1H1 RING E3 ubiquitin ligase, RING membrane-anchor 1 homologue 1 (Park et al. 2003; Lee

et al. 2009), a ribosomal protein alanine, encoding an Acyl-CoA N-acyltransferase (NAT) superfamily protein similar to the histone acetyltransferase GCN5 (Chen and Tian 2007), a member of the Major Facilitator Superfamily, encoding a sugar transporter of the polyol/monosaccharide transporter (PMT) family (Kiyosue et al. 1998; Wormit et al. 2006; Aluri and Buettner 2007; Yamada et al. 2010) and a WRKY transcription factor with homology to stress-response-associated WRKY28 (Wu et al. 2011) and WRKY8 (Hu et al. 2013). Genes located off of the left border of the T-DNA insertion in *nikku* also showed some expression modification (genes encoding a GDSL esterase/lipase and a serine/threonine protein phosphatase similar to protein phosphatase PP7), and these genes are also associated with stress response (Liu et al. 2007; Hong et al. 2008; Jiang et al. 2012). Furthermore, several of these genes, based on the biological functions of their encoded proteins (E3 ubiquitin ligase, histone acetyltransferase, transcription factor, protein phosphatase), would be expected to have effects on various other downstream genes and/or proteins, further contributing to signaling within the mutant and the overall *nikku* phenotype.

An interesting feature of this study was the unexpected appearance of the partial revertant phenotype, which appeared during routine subculture. While revertants have not been commonly reported in activation tagging studies,

Weigel et al. (2000) reported that several Arabidopsis mutant lines generated using the same pSKI074 vector became attenuated in subsequent generations, with a reversion to wild-type phenotype. This was attributed to the selective inactivation of the CaMV 35S enhancers, but no corresponding analysis of the enhancer sequences was provided. Our initial thoughts were that the instability of the 35S enhancer elements could be the cause for reversion. However, our analyses of the revertant phenotype plants indicated that the T-DNA structure and integration site was intact and the reversion of the *nikku* phenotype was not due to enhancer loss. An alternative explanation may be that some tissue culture-induced mutation may have occurred in *nikku*, leading to the revertant phenotype.

If we considered the 35S enhancer elements themselves, it is possible that epigenetic modification via methylation of the transgene had taken place, with an effect on the activation tag effectiveness. Vectors consisting of enhancers derived from the CaMV promoters (e.g., pSKI074) are commonly used in activation tagging, and the pSKI074 vector was first used to generate gain-of-function mutants in Arabidopsis (Weigel et al. 2000). In activation-tagged mutants, the methylation of enhancer sequences may reduce their ability to over-express adjacent native genes, thereby eliminating the visible phenotype. The low frequency of visible phenotypes of dominant gain-of-function mutants generated using activation tagging vector pSKI074 has been attributed to the methylation of enhancer sequences (Chalfun-Junior et al. 2003) in multiple insertions.

Our experimental data from methylated DNA PCR analysis of the enriched methylated DNA fraction for *nikku* and the revertant suggested that differential methylation may be involved, with distinct differences in the level of 35S enhancer cytosine methylation between the two. However, our observations of hypo-methylation of the 35S tetramer enhancer regions of the revertant in comparison to *nikku* are in contrast to the observations of Mishiba et al. (2010), which associate 35S enhancer hyper-methylation with enhancer gene silencing. These authors identified a consensus target region for de novo methylation of the 35S promoter, with distinct footprints associated with the 35S promoter and the enhancer region crucial for methylation. However, tetramerized 35S enhancers were not analyzed in that study. Hence, it is not known how the pattern of cytosine methylation might change in this tetramerized enhancer context during silencing. The methodology used in our study allowed for the detection of overall methylation levels in single 35S enhancers amplified by PCR, but did not allow us to determine site-specific methylation differences between *nikku* and the revertant. In addition, our methodology also did not allow us to determine the pattern of cytosine methylation in the ordered series of 35S enhancers comprising the tetramer for *nikku* and revertant.

Therefore, it is possible that a reduced effect of 35S enhancers in the revertant was a result of variation in methylation of specific cytosine residues, rather than the overall reduced level of methylation. Future work will look to assess site-specific methylation of the enhancer elements in *nikku* and the revertant, via bisulfite sequencing.

The global quantification of DNA methylation can also provide insight into the mutant and revertant genotypes compared to local 35S enhancer methylation. Whole genome DNA hypo-methylation is closely associated with several developmental abnormalities, altered stress response, gene expression changes and chromatin re-arrangements (Kakutani et al. 1996; Santos et al. 2011). In the present study, we observed the global hypo-methylation of *nikku* DNA to a level approximately 50 % less than that of the wild-type Bintje, indicating that the severely stressed mutant phenotype was associated with this change in methylation. It is worth noting that the level of cytosine methylation in revertant phenotype plants is significantly greater than for *nikku*, but still less than wild-type Bintje plants (Fig. 11), suggesting that the partial reversion phenotype was also associated with a partial reversion to more wild-type cytosine methylation levels. Also, taking into account the change in gene expression levels and phenotypic appearance of revertant phenotype plants, we believe that phenotype, gene expression and DNA methylation levels are intertwined. For example, the Arabidopsis *ddm1* (decrease in DNA methylation 1) mutant, closely resembles the *nikku* phenotype, with reduced apical dominance, twisted leaves, small plant size, etc. (Kakutani et al. 1996). Furthermore, in hypo-methylated tobacco plants 16 genes (out of 30) related to stress response were up-regulated (Wada et al. 2004) indicating a relationship between plant stress and hypo-methylation.

The importance of cytosine methylation for plant development has been demonstrated by the treatment of plants with the hypo-methylating agent, zebularine (Baubec et al. 2009; Malik et al. 2012). Our use of zebularine with potato explants provided further evidence for the involvement of DNA cytosine methylation in the *nikku* phenotype. When Bintje, *nikku* and revertant shoots were cultured on media containing zebularine, both Bintje and the revertant came to resemble the phenotype of the *nikku* mutant. Interestingly, increasing concentrations of zebularine did not seem to have any impact on the severe phenotype associated with *nikku*, suggesting that *nikku* may already represent the maximal severe stress phenotype and hypo-methylation possible. Our study indicated that the level of cytosine methylation in *nikku* was 50 % that of Bintje. In the study by Malik et al. (2012) with *Physcomitrella patens*, increasing zebularine concentrations resulted in delayed and abnormal differentiation, as well as stunted growth. The maximal reduction in cytosine

methylation obtained was approximately 50 % that of control, and increasing concentrations of zebularine could not reduce this level of methylation any further. Therefore, this 50 % reduction in DNA methylation, such as we observed with *nikku* and Malik et al. (2012) observed through zebularine applications, may represent a limiting level.

This paper has characterized a novel potato mutant, *nikku*, generated via activation tagging, which exhibits a severe stress phenotype, as well as an interesting revertant phenotype. Numerous genes flanking the *nikku* T-DNA insertion (and, we must assume, across the whole genome) were modified in their expression profiles, with many associated with stress-response pathways. Furthermore, *nikku* was also characterized by a 50 % reduction in DNA cytosine methylation levels, while Bintje and revertant gene expression and methylation levels were more similar to each other. We are unsure if any of the single genes identified flanking the T-DNA insertion underlies the *nikku* phenotype, and what role DNA cytosine methylation plays in this overall phenotype. However, the variations in gene expression and methylation status observed in the mutant, as related to the wild-type Bintje and revertant phenotype plants, are expected to contribute to the mutant phenotype. The complex gene expression patterns observed for *nikku* and the revertant, and the added layers of methylation and stress-induced gene expression, make *nikku* and the revertant an interesting crop plant system with which to study the relationship between severe stress, DNA methylation and plant growth.

Author contribution BSF, RV and SSA conceived and designed the research. SSA conducted the majority of the experiments and analysis, while GT carried out the GenomeWalker experiments and analysis. SSA, BSF and RV wrote the manuscript.

References

Ahn JH, Kim J, Yoo SJ, Yoo SY, Roh H, Choi JH, Choi MS, Chung KS, Han EJ, Hong SM, Jung SH, Kang HJ, Kim BK, Kim MD, Kim YK, Kim YH, Lee H, Park SH, Yang JH, Yang JW, Yoo DH, Yoo SK, Lee JS (2007) Isolation of 151 mutants that have developmental defects from T-DNA tagging. Plant Cell Physiol 48:169–178

Aluri S, Buettner M (2007) Identification and functional expression of the *Arabidopsis thaliana* vacuolar glucose transporter 1 and its role in seed germination and flowering. Proc Natl Acad Sci USA 104:2537–2542

Aulakh SS, Veilleux RE, Dickerman AW, Tang G, Flinn BS (2014) Characterization and RNA-seq analysis of *underperformer*, an activation-tagged potato mutant. Plant Mol Biol 84:635–658

Ayliffe MA, Pryor AJ (2007) Activation tagging in plants—generation of novel, gain-of-function mutations. Aust J Agr Res 58:490–497

Ayliffe MA, Pallotta M, Langridge P, Pryor AJ (2007) A barley activation tagging system. Plant Mol Biol 64:329–347

Baubec T, Pecinka A, Rozhon W, Mittelsten Scheid O (2009) Effective, homogeneous and transient interference with cytosine methylation in plant genomic DNA by zebularine. Plant J 57:542–554

Borevitz JO, Xia YJ, Blount J, Dixon RA, Lamb C (2000) Activation tagging identifies a conserved MYB regulator of phenyl-propanoid biosynthesis. Plant Cell 12:2383–2393

Busov VB, Meilan R, Pearce DW, Ma CP, Rood SB, Strauss SH (2003) Activation tagging of a dominant gibberellin catabolism gene (*GA 2-oxidase*) from poplar that regulates tree stature. Plant Physiol 132:1283–1291

Busov V, Yordanov Y, Gou JQ, Meilan R, Ma C, Regan S, Strauss S (2011) Activation tagging is an effective gene tagging system in *Populus*. Tree Genet Genom 7:91–101

Chalfun-Junior A, Mes JJ, Mlynarova L, Aarts MGM, Angenent GC (2003) Low frequency of T-DNA based activation tagging in *Arabidopsis* is correlated with methylation of CaMV 35S enhancer sequences. FEBS Lett 555:459–463

Chen ZJ, Tian L (2007) Roles of dynamic and reversible histone acetylation in plant development and polyploidy. BBA Gene Struct Expr 1769:295–307

Gopal J, Chamail A, Sarkar D (2004) In vitro production of microtubers for conservation of potato germplasm: effect of genotype, abscisic acid, and sucrose. In Vitro Cell Dev Plant 40:485–490

Hayashi H, Czaja I, Lubenow H, Schell J, Walden R (1992) Activation of a plant gene by T-DNA tagging: auxin-independent growth in vitro. Science 258:1350–1353

He CK, Dey M, Lin ZH, Duan FP, Li FL, Wu R (2007) An efficient method for producing an indexed, insertional-mutant library in rice. Genomics 89:532–540

Hong JK, Choi HW, Hwang IS, Kim DS, Kim NH, Choi DS, Kim YJ, Hwang BK (2008) Function of a novel GDSL-type pepper lipase gene, CaGLIP1, in disease susceptibility and abiotic stress tolerance. Planta 227:539–558

Hsing YI, Chern CG, Fan MJ, Lu PC, Chen KT, Lo SF, Sun PK, Ho SL, Lee KW, Wang YC, Huang WL, Ko SS, Chen S, Chen JL, Chung CI, Lin YC, Hour AL, Wang YW, Chang YC, Tsai MW, Lin YS, Chen YC, Yen HM, Li CP, Wey CK, Tseng CS, Lai MH, Huang SC, Chen LJ, Yu SM (2007) A rice gene activation/knockout mutant resource for high throughput functional genomics. Plant Mol Biol 63:351–364

Hu Y, Chen L, Wang H, Zhang L, Wang F, Yu D (2013) *Arabidopsis* transcription factor WRKY8 functions antagonistically with its interacting partner VQ9 to modulate salinity stress tolerance. Plant J 74:730–745

Imaizumi R, Sato S, Kameya N, Nakamura I, Nakamura Y, Tabata S, S-i Ayabe, Aoki T (2005) Activation tagging approach in a model legume, *Lotus japonicus*. J Plant Res 118:391–399

Ito T, Motohashi R, Kuromori T, Noutoshi Y, Seki M, Kamiya A, Mizukado S, Sakurai T, Shinozaki K (2005) A resource of 5,814 dissociation transposon-tagged and sequence-indexed lines of *Arabidopsis* transposed from start loci on chromosome 5. Plant Cell Physiol 46:1149–1153

Jeong DH, An SY, Kang HG, Moon S, Han JJ, Park S, Lee HS, An KS, An GH (2002) T-DNA insertional mutagenesis for activation tagging in rice. Plant Physiol 130:1636–1644

Jiang Y, Chen R, Dong J, Xu Z, Gao X (2012) Analysis of GDSL lipase (GLIP) family genes in rice (*Oryza sativa*). Plant Omics 5:351–358

Jungkunz I, Link K, Vogel F, Voll LM, Sonnewald S, Sonnewald U (2011) AtHsp70-15-deficient *Arabidopsis* plants are characterized by reduced growth, a constitutive cytosolic protein response and enhanced resistance to TuMV. Plant J 66:983–995

Kakutani T, Jeddeloh JA, Flowers SK, Munakata K, Richards EJ (1996) Developmental abnormalities and epimutations associated with DNA hypomethylation mutations. Proc Natl Acad Sci USA 93:12406–12411

Kardailsky I, Shukla VK, Ahn JH, Dagenais N, Christensen SK, Nguyen JT, Chory J, Harrison MJ, Weigel D (1999) Activation tagging of the floral inducer FT. Science 286:1962–1965

Kiyosue T, Abe H, Yamaguchi-Shinozaki K, Shinozaki K (1998) ERD6, a cDNA clone for an early dehydration-induced gene of *Arabidopsis*, encodes a putative sugar transporter. BBA Biomembranes 1370:187–191

Krysan PJ, Young JC, Sussman MR (1999) T-DNA as an insertional mutagen in *Arabidopsis*. Plant Cell 11:2283–2290

Larkin MA, Blackshields G, Brown NP, Chenna R, McGettigan PA, McWilliam H, Valentin F, Wallace IM, Wilm A, Lopez R, Thompson JD, Gibson TJ, Higgins DG (2007) Clustal W and clustal X version 2.0. Bioinformatics 23:2947–2948

Lee HK, Cho SK, Son O, Xu Z, Hwang I, Kim WT (2009) Drought stress-induced Rma1H1, a RING membrane-anchor E3 ubiquitin ligase homolog, regulates aquaporin levels via ubiquitination in transgenic *Arabidopsis* plants. Plant Cell 21:622–641

Liu HT, Li GL, Chang HUI, Sun DY, Zhou RG, Li B (2007) Calmodulin-binding protein phosphatase PP7 is involved in thermotolerance in *Arabidopsis*. Plant, Cell Environ 30:156–164

Malik G, Dangwal M, Kapoor S, Kapoor M (2012) Role of DNA methylation in growth and differentiation in *Physcomitrella patens* and characterization of cytosine DNA methyltransferases. FEBS J 279:4081–4094

Marsch-Martinez N, Greco R, Van Arkel G, Herrera-Estrella L, Pereira A (2002) Activation tagging using the *En-I* maize transposon system in *Arabidopsis*. Plant Physiol 129:1544–1556

Mathews H, Clendennen SK, Caldwell CG, Liu XL, Connors K, Matheis N, Schuster DK, Menasco DJ, Wagoner W, Lightner J, Wagner DR (2003) Activation tagging in tomato identifies a transcriptional regulator of anthocyanin biosynthesis, modification, and transport. Plant Cell 15:1689–1703

Mishiba KI, Yamasaki S, Nakatsuka T, Abe Y, Daimon H, Oda M, Nishihara M (2010) Strict de novo methylation of the 35S enhancer sequence in gentian. PLoS One 5(3):e9670

Miyao A, Iwasaki Y, Kitano H, Itoh J, Maekawa M, Murata K, Yatou O, Nagato Y, Hirochika H (2007) A large-scale collection of phenotypic data describing an insertional mutant population to facilitate functional analysis of rice genes. Plant Mol Biol 63:625–635

Murashige T, Skoog F (1962) A revised medium for rapid growth and bioassays with tobacco tissue cultures. Physiol Plant 15:473–497

Park JA, Cho SK, Kim JE, Chung HS, Hong JP, Hwang B, Hong CB, Kim WT (2003) Isolation of cDNAs differentially expressed in response to drought stress and characterization of the *Ca-LEAL1* gene encoding a new family of atypical LEA-like protein homologue in hot pepper (*Capsicum annuum* L. cv. *Pukang*). Plant Sci 165:471–481

Regan S, Gustafson V, Rothwell C, Sardana R, Flinn B, Mallubhotla S, Bagchi M, Siahbazi M, Chakravarty B, Wang-Pruski G, Goyer C, Audy P, Li X-Q, De Koeyer D (2006) Finding the perfect potato: using functional genomics to improve disease resistance and tuber quality traits. Can J Plant Path 28:S247–S255

Rubtsov MA, Polikanov YS, Bondarenko VA, Wang YH, Studitsky VM (2006) Chromatin structure can strongly facilitate enhancer action over a distance. Proc Natl Acad Sci USA 103:17690–17695

Santos AP, Ferreira L, Maroco J, Oliveira MM (2011) Abiotic stress and induced DNA hypomethylation cause interphase chromatin structural changes in rice rDNA loci. Cytogenet Genome Res 132:297–303

Silva JAB, Otoni WC, Martinez CA, Dias LM, Silva MAP (2001) Microtuberization of Andean potato species (*Solanum* spp.) as affected by salinity. Sci Hortic 89:91–101

Suzuki Y, Uemura S, Saito Y, Murofushi O, Schmitz G, Theres K, Yamaguchi I (2001) A novel transposon tagging element for obtaining gain-of-function mutants based on a self-stabilizing Ac derivative. Plant Mol Biol 45:123–131

The Potato Genome Sequencing Consortium (2011) Genome sequence and analysis of the tuber crop potato. Nature 475:189–194

van der Graaff E, Den Dulk-Ras A, Hooykaas PJJ, Keller B (2000) Activation tagging of the *LEAFY PETIOLE* gene affects leaf petiole development in *Arabidopsis thaliana*. Development 127:4971–4980

van der Graaff E, Nussbaumer C, Keller B (2003) The *Arabidopsis thaliana rlp* mutations revert the ectopic leaf blade formation conferred by activation tagging of the *LEP* gene. Mol Genet Genomics 270:243–252

Veilleux RE, Mills KP, Baxter AJ, Upham KT, Ferguson TJ, Holt SH, Lu N, Ruiz-Rojas JJ, Pantazis CJ, Davis CM, Lindsay RC, Powell FL, Dan Y, Dickerman AW, Oosumi T, Shulaev V (2012) Transposon tagging in diploid strawberry. Plant Biotechnol J 10:985–994

Wada Y, Miyamoto K, Kusano T, Sano H (2004) Association between up-regulation of stress-responsive genes and hypomethylation of genomic DNA in tobacco plants. Mol Genet Genomics 271:658–666

Walden R, Fritze K, Hayashi H, Miklashevichs E, Harling H, Schell J (1994) Activation tagging—a means of isolating genes implicated as playing a role in plant growth and development. Plant Mol Biol 26:1521–1528

Weigel D, Ahn JH, Blazquez MA, Borevitz JO, Christensen SK, Fankhauser C, Ferrandiz C, Kardailsky I, Malancharuvil EJ, Neff MM, Nguyen JT, Sato S, Wang ZY, Xia YJ, Dixon RA, Harrison MJ, Lamb CJ, Yanofsky MF, Chory J (2000) Activation tagging in *Arabidopsis*. Plant Physiol 122:1003–1013

Williams ME, Torabinejad J, Cohick E, Parker K, Drake EJ, Thompson JE, Hortter M, DeWald DB (2005) Mutations in the *Arabidopsis* phosphoinositide phosphatase gene *SAC9* lead to overaccumulation of PtdIns(4,5)P-2 and constitutive expression of the stress-response pathway. Plant Physiol 138:686–700

Wormit A, Trentmann O, Feifer I, Lohr C, Tjaden J, Meyer S, Schmidt U, Martinoia E, Neuhaus HE (2006) Molecular identification and physiological characterization of a novel monosaccharide transporter from *Arabidopsis* involved in vacuolar sugar transport. Plant Cell 18:3476–3490

Wu LT, Zhong GM, Wang JM, Li XF, Song X, Yang Y (2011) *Arabidopsis* WRKY28 transcription factor is required for resistance to necrotrophic pathogen, *Botrytis cinerea*. Afr J Microbiol Res 5:5481–5488

Yamada K, Osakabe Y, Mizoi J, Nakashima K, Fujita Y, Shinozaki K, Yamaguchi-Shinozaki K (2010) Functional analysis of an *Arabidopsis thaliana* abiotic stress-inducible facilitated diffusion transporter for monosaccharides. J Biol Chem 285:1138–1146